Developing a Cost-Effective Multispectral Imaging System for Real-Time Nuclear Fuel Pellet Inspection

R. David Dunphy (University of Strathclyde), Manuel Bandala (Lancaster University), Patrick Chard (Mirion Technologies), Neil Cockbain (National Nuclear Laboratory),
David Eaves (Westinghouse), Paul R. Edwards (University of Strathclyde), Daniel Hutchinson (Westinghouse), Xiandong Ma (Lancaster University),
Stephen Marshall (University of Strathclyde), Robert W. Martin (University of Strathclyde), Paul Murray (University of Strathclyde), Andrew J. Parker (Lancaster University),
Paul Stirzaker (Westinghouse), C. James Taylor (Lancaster University), Jaime Zabalza (University of Strathclyde), Malcolm Joyce (Lancaster University)

1. Introduction

The production of nuclear fuel is a complex and multi-staged manufacturing process in which UF_6 is converted to UO_2 powder, compressed into pellet form, and sintered into a solid ceramic form.

Fig. 1. Nuclear fuel pellets during production

To ensure compliance of the nuclear fuel with specification, pellets are manually assessed in terms of fuel enrichment, pellet dimensional consistency, and surface defects and contaminants. Deviation from specification is only detected following manufacture of an entire batch of fuel, which then needs to be recycled, costing significant time and monetary resources.

In this project, we aim to investigate whether this assessment can be carried out continuously throughout the process using a spectral imaging system, with the aim of making the manufacturing process more responsive. Hyperspectral imaging (HSI) has been successfully used to characterise UO_2 pellets [1], identifying useful spectral regions in the short-wave infrared (SWIR) range. Based on the hyperspectral findings, we develop a low-cost multispectral imaging (MSI) system suitable for deployment in radiological contamination areas.

2. Hyperspectral data acquisition

A bespoke turntable (Fig. 2a: 1) and pellet roller stage (2) were constructed to enable simultaneous data acquisition using gamma-ray spectroscopy (3), laser profilometry (4), RGB data (5) and SWIR hyperspectral data (6). Pellets are illuminated using a broad-band illumination source (7). The roller stage is designed to manipulate AGR pellets (8) using a pair of motorised rollers (9). Angled mirrors (10) allow the ends to be imaged [2].

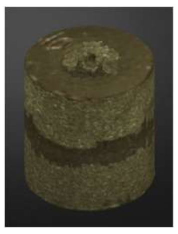

Fig. 2b. Reconstructed AGR pellet model

This results in 360° data acquisition. Laser profilometry and imaging data are fused to create a 3D reconstruction of the pellet for defect detection. Three datasets of pellets imaged from different sources were obtained. A: 16 AGR pellets (Fig. 2b); B: 8 UO_2 and SimFuel pellets; C: 20 UO_2 pellets doped with simulated fission products.

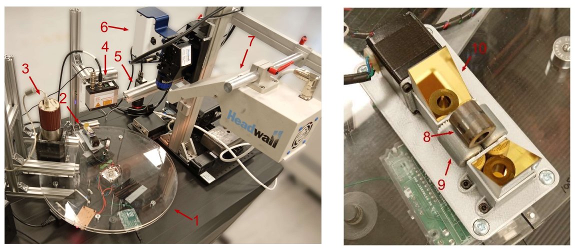

Fig. 2a. 360° pellet imaging turntable and roller stage set-up

3. Spectral analysis

Hyperspectral images of UO_2 pellets are calibrated to a Spectralon tile using one-point calibration. To reduce lighting artefacts and scatter effects, spectra are normalised using a method proposed by Barnes *et al.* [3], in which the quadratic trend of absorbance Q_A is subtracted in absorbance space:

$$\hat{R} = 10^{Q_A + \log_{10} R}$$

Fig. 3a shows spectral features obtained for 16 pure UO_2 AGR pellets. Spectral features are distinctive and repeatable across datasets.

A comparison with pellets doped with simulated fission products (Fig. 3b) indicates spectral features may be useful for spent fuel analysis.

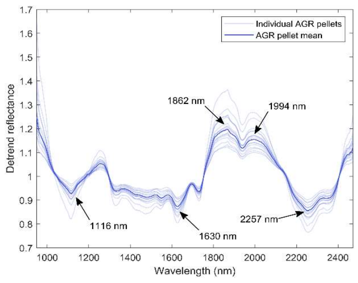

Fig. 3a. Spectral features in UO_2 AGR pellets

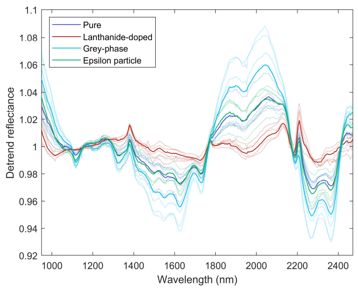

Fig. 3b. SimFuel doped pellet spectra

4. Spectral similarity metrics

A spectral index derived from the magnitude of the main spectral feature at 1870 nm is proposed, and defined as:

$$Z = \frac{\hat{R}_{1870\,\mathrm{nm}} - \hat{R}_{2257\,\mathrm{nm}}}{\max_{\lambda} \hat{R} - \min_{\lambda} \hat{R}}$$

This score clearly separates lanthanide-doped pellets from other pellet classes (Fig. 4a). Fig. 4b shows the spatial distribution of these scores.

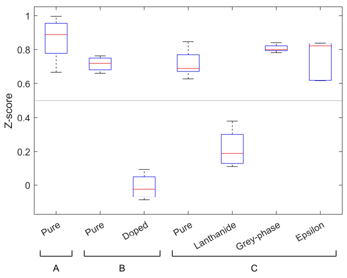

Fig. 4a. Z-score values for pellet classes

Fig. 4c shows the pairwise spectral information divergence (SID) for each pair of classes, confirming that the SimFuel and lanthanide-doped pellets are more similar to each other than to other classes.

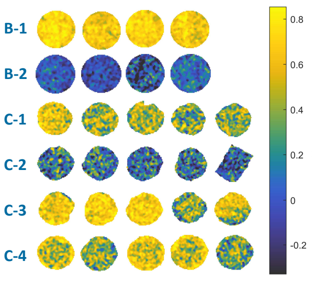

Fig. 4b. Spatial distribution of Z-scores

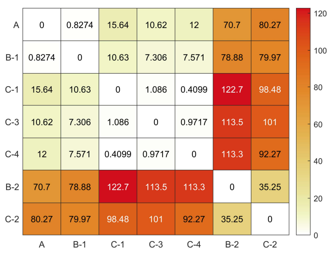

	A	B-1	C-1	C-3	C-4	B-2	C-2
A	0	0.8274	15.64	10.62	12	70.7	80.27
B-1	0.8274	0	10.63	7.306	7.571	78.88	79.97
C-1	15.64	10.63	0	1.086	0.4099	122.7	98.48
C-3	10.62	7.306	1.086	0	0.9717	113.5	101
C-4	12	7.571	0.4099	0.9717	0	113.3	92.27
B-2	70.7	78.88	122.7	113.5	113.3	0	35.25
C-2	80.27	79.97	98.48	101	92.27	35.25	0

Fig. 4c. Pairwise SID scores for pellet classes

5. Multispectral imaging as a low-cost alternative to SWIR HSI

Due to the risk of radiological contamination, a low-cost alternative to hyperspectral imaging is desired for production line testing. We propose a custom multispectral system based on the findings of our hyperspectral analysis. In addition to reducing cost, the use of a multispectral camera allows for faster data acquisition without sacrificing the spatial resolution needed to detect physical defects such as chips, cracks, and irregularities in the geometry of the fuel pellets, which is advantageous due to the high number of pellets produced.

The proposed system consists of an InGaAs sensor (900 nm to 1700 nm), a filter wheel with 10 bandpass filters (Fig. 5a), and a halogen ring-light. The assembled system, shown in Fig. 5b, can be mounted vertically above samples, and has a nominal imaging distance of 110 mm. Bandpass filters are selected from a range of off-the-shelf options to align with spectral features observed in the hyperspectral data (Fig. 5c), with a FWHM of between 12 nm and 50 nm. The reduced spectral range of the sensor relative to the MCT hyperspectral sensor (950 nm to 2500 nm) necessitates focussing on smaller features.

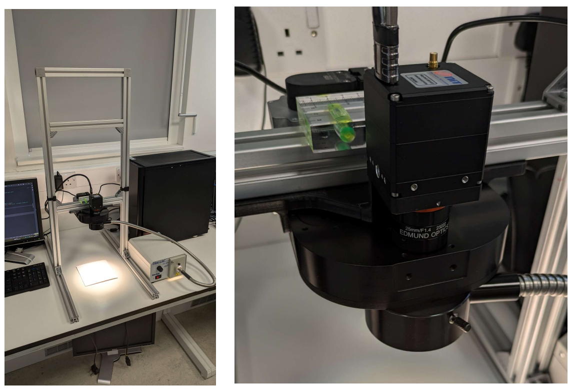

Fig. 5b. Assembled MSI system

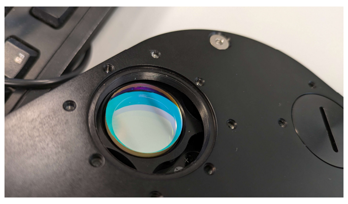

Fig. 5a. Filter wheel with band pass filter

The expected MSI response was simulated by integrating the spectral profile over each filter transmission spectrum (Fig. 5d). The simulated results suggest that the system should be capable of observing spectral features at 1125 nm, 1325 nm, and 1625 nm.

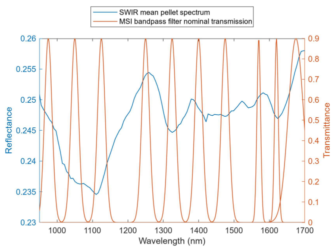

Fig. 5c. MSI filter responses over UO_2 spectrum

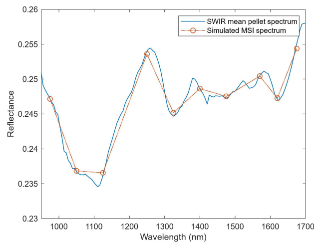

Fig. 5d. Simulated MSI response

6. MSI data acquisition and results

As Fig. 6a shows, the aperture used affects the depth of field of the camera. Since the focal distance varies with wavelength, this also introduces chromatic effects where channels at the extremes of the sensors wavelength range are not in focus at the same distances. To minimise these effects, images were captured at f8, with an exposure time of 24 ms (48 ms for channels 8 to 10, which have narrower bandwidths).

A dataset of 108 images of pellets from groups B and C was compiled, a selection of which are shown in Fig. 6b, including pellets submerged in 10 mm of de-ionised water (Fig. 6c), which are of interest for spent fuel analysis. Fig. 6d shows an example mean spectral signature obtained for a pure UO_2 pellet, compared with the simulated spectrum calculated from the SWIR data. Due to the reduced spectral resolution, quadratic detrending does not perform well on this data, so we use the standard normal variate (SNV).

Fig. 6b. False-colour images from channels 4, 3, and 2 of MSI data for UO_2 pellets

The 1116 nm absorbance band can clearly be observed by indexing channels 3 and 4 of the normalised data, and is responsible for the red colouration of the false-colour images. An additional feature around 1325 nm is also discernible, but the 1630 nm feature is lost due to high noise levels in the image data. Longer exposure times are necessary to compensate for this.

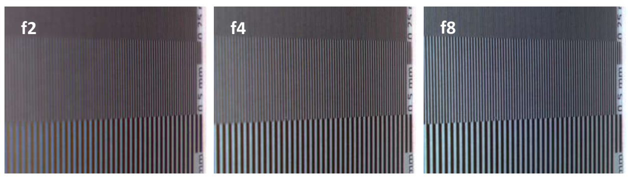

Fig. 6a. Small apertures increase depth of field and reduce chromatic effects

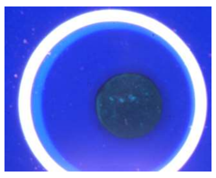

Fig. 6c. Pellet in de-ionised water

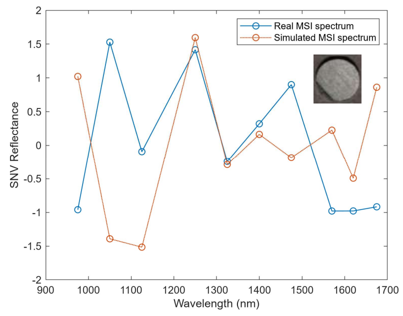

Fig. 6d. Mean SNV spectrum for sample pellet

7. Conclusions

- Hyperspectral analysis of nuclear fuel pellets has determined characteristic absorbance features in sintered UO_2.
- Comparing the spectra of pure pellets with those of pellets doped with contaminants indicates that HSI can be used for QA.
- A multispectral system is developed to enable simultaneous detection of physical defects and chemical contamination.
- Initial results indicate that an absorbance band at 1116 nm can be detected using the 1125 nm filter of the MSI system.
- Future work will focus on field-testing and validating the system's performance in a production environment.

References

[1] J. Zabalza *et al.*, "Hyperspectral imaging based characterization and identification of sintered UO_2 fuel pellets," *2023 IEEE Nuclear Science Symposium (NSS), Medical Imaging Conference (MIC) and Room Temperature Semiconductor Detector Conference (RTSD)*, 2023, doi: 10.1109/NSSMICRTSD49126.2023.10338358.

[2] A. Parker *et al.*, "A prototype multi-instrument quality assurance system for responsive nuclear fuel manufacturing," *2024 IEEE Nuclear Science Symposium (NSS), Medical Imaging Conference (MIC) and Room Temperature Semiconductor Detector Conference (RTSD)*, 2024, doi: 10.1109/NSS/MIC/RTSD57108.2024.10656207.

[3] R. J. Barnes *et al.*, "Standard normal variate transformation and de-trending of near-infrared diffuse reflectance spectra," *Applied Spectroscopy*, 1989, doi: 10.1366/0003702894202201.